Int. J. of Geosynth. and Ground Eng. (2016) 2:28
DOI 10.1007/s40891-016-0064-4

ORIGINAL ARTICLE

Unconfined Compressive Strength of Compacted Disturbed Cement-Stabilized Soft Clay

Mohamed Ayeldeen[1] · Yuki Hara[2] · Masaki Kitazume[2] · Abdelazim Negm[3]

Received: 26 May 2016 / Accepted: 19 July 2016 / Published online: 26 September 2016

Abstract Pneumatic flow mixing method is a new land reclamation method, developed in Japan to meet the persistent lack of space. In this method dredged soft soil is mixed with a small amount of stabilizing material (such as cement) during transporting the soft soil in a pipe using compressed air to be used for land reclamation. In some cases, the soil/cement mixture is stored in temporary place for days and then transported and compacted at the required place. Basically, the cement chemical reaction starts immediately after the mixing with the soft soil and the mixture starts to gain its strength, therefore disturbing the mixture after days from the mixing influences the mixture strength. However, the soil/cement mixture is still able to gain extra strength after disturbance, transportation, and compaction. This study aims to evaluate the effect of dynamic compaction on the shear strength of disturbed cemented soft soil mixture experimentally. The mixture was fully disturbed after one week from mixing with cement. Three cement/soil ratios were used in this study under different dynamic compaction energies. Unconfined compression test was conducted at various curing times for both disturbed and non-disturbed specimens.

Keywords Pneumatic flow mixing · Stabilized soft clay · Compaction · Unconfined compressive strength · Soil disturbance

List of Symbols

aw	Cement ratio
E_{50}	Modulus of deformation
t	Curing time
q_{un}	Unconfined compressive strength
q_{un_Non}	Unconfined compressive strength for non-disturbed cemented clay
$q_{un\_Non\_t}$	Unconfined compressive strength for non-disturbed cemented clay at curing time t
q_{un_D}	Unconfined compressive strength for disturbed cemented clay
$q_{un\_D\_T}$	Unconfined compressive strength for disturbed cemented clay without compaction
$q_{un\_D\_T\_t}$	Unconfined compressive strength for disturbed cemented clay without compaction at curing time t
$q_{un\_D\_comp}$	Unconfined compressive strength for compacted disturbed cemented clay
$q_{un\_D\_comp\_t}$	Unconfined compressive strength for compacted disturbed cemented clay at curing time
i	Increasing factor ($i = q_{un\_D\_comp\_t}/q_{un\_D\_T\_28}$)
G_s	Average specific gravity for the specimen
γ_w	Water unit weight
γ_t	Total unit weight after curing
γ_d	Dry unit weight after curing
e	Void ratio after curing time
R^2	Coefficient of determination

✉ Mohamed Ayeldeen
ayeldeen@f-eng.tanta.edu.eg

[1] Structural Engineering Department, Faculty of Engineering, Tanta University, Tanta, Egypt

[2] Civil and Environmental Engineering Department, Tokyo Institute of Technology, Tokyo, Japan

[3] Civil Engineering Department, Faculty of Engineering, Zagazig University, Zagazig, Egypt

Introduction

Soft soil deposits can be found in many places all over the world especially coastal areas, which are recognized by the high compressibility and low shear strength. Where it became essential to find appropriate method to improve the softy soil characterizations to meet the needed engineering requirements for construction. One of the new methods used to improve the soft soil for land reclamation is pneumatic flow mixing method, which depends on mixing the dredged soft soil with cement during transporting the soil through pipes to the construction site [1–4]. However, in some cases the soil/cement mixture has to be stored in other place for days and then transported again to the construction site. In that case the soil/cement mixture become disturbed, where the cement chemical reaction already started as soon as the cement has been mixed with the soil. The disturbance process, which is necessary to transport the mixture after days to the site, shall change the mixture behaviour especially after using compaction to place the mixture in its final site [5].

At the beginning, mixing the clay with cement destroy the natural clay cementation between the clay particles and replace that with cement admixed clay. Many investigations have been done to understand the behaviour of cement admixed clay under different variables such as water content, cement ratio, and curing time [6–18]. It was revealed that the strength and deformation characterizations are manly depending on the fabric (clay cluster) and the cementation, while the main role for cementation is to weld the clay particles together after destroying the natural cementation. The shear strength increases with increasing the bond between the particles which depending on different factor such as cement ratio and curing time [6].

For some cases of *pneumatic flow mixing method*, the cemented soft clay has to be transported from its initial place to the construction site after several days. In this case, disturbing the soil shall breakdown the welding connections formed between the particles, however another connection shall form again after setting up and compacting the soil in the final site. Hence the chemical reaction of the cement already started once the cement has been mixed with the soil, the efficiency of the connections reformed after the disturbance is affected by the time period spent from mixing paste till the disturbance and setting up again. The longer this period is, the weaker this reformed connection will be. In this study the disturbed period has chosen to be as long as possible, to represent optimum reduction of the soil strength after disturbance, where the chosen period is 7 days from mixing the paste till the disturbance and the molding. According to the literature, the cement mixture gains about 65–75 % of its nominated strength (nominated strength is the strength after 28 curing days) after 7 days, i.e. the disturbance after 7 days will breakdown about 65–75 % from the formed connections [19, 20]. However, even after disturbing the paste, the pervious cemented formed elements attached to the clay particles shall still help to increase the final shear strength. The remaining chemical cement chemical reaction shall also help in increasing the final shear strength of the paste, especially with the effect of compaction which will reduce the gaps between the soil particles and helping the formation of new connections. For soft clay improvement, normally, the clay mix with medium to high cement ratio. The mean effective yield stress of the cemented clay is higher than the confining pressure developed from the overburden pressure and external loads, therefore the induced cementation will be the major responsible of the shear resistance. Thus, using unconfined compression strength shall be appropriate to study the behaviour of the compacted cement-stabilized soft clay [7].

This study is an attempt to understand and evaluate the unconfined compressive strength of compacted disturbed cement-stabilized soft clay. Three cement/clay ratios were used in this study (5, 10 and 15 %). Different compaction energies were used to compact the disturbed soil, while tapping was used for non-disturbed soil. Unconfined compression test was performed for both disturbed and non-disturbed specimens after different curing times. Artificial Neural network model was developed to correlate the increasing in compressive stress due to the effect of compaction energy and curing time.

Materials and Test Procedure

Material Properties and Specimen Preparation

In order to have a clear understanding of the effect of compaction on the mechanical properties of disturbed cement-stabilized soft clay, Kaolin clay (w_L of 77.5 % and w_P of 30.3 %) and ordinary Portland cement were used in this study. Kaolin clay was mixed with tap water for one hour in a vacuum mixer at a water content ratio of 120 %. Ordinary Portland cement was added after to the slurry at cement content varying from 5 to 15 %, and both clay slurry and ordinary Portland cement were mixed for 10 min. Cement content, *aw*, can be defined as the ratio between the weight of cement and the weight of clay in dry case. The paste was then split in two parts (one part for non-disturbed specimens and the other for disturbed specimens). For non-disturbed specimens, the paste was used immediately after mixing and molded by tapping in a

plastic mold, 50 mm diameter and 100 mm height at three layers [21]. Each layer was tapped 100 times to grantee the homogeneity of the specimens. The non-disturbed specimens were kept in humidity curing chamber and were tested after 7, 28, 35 and 42 days from mixing the paste.

For disturbed specimens, the paste was kept airtight in plastic bag for 7 days before it fully disturbed for 5 min in the mechanical mixer. Specimens were molded in the same plastic molds as in the non-disturbed case, however various dynamic compaction energies were used to mold the disturbed specimens. The molds were filled at three layers; each layer was dynamically compacted by 1 kg cylinder hummer falling free from a height of 1 m. Different numbers of blows (5, 10, 20 and 40) were used to compact each layer to obtain different compaction energies. The tapping technique was also used to compact disturbed specimens at compaction energy of zero. The specimens were kept also in humidity curing chamber and were tested after 28, 35 and 42 days from the initial mixing.

Test Procedure

Unconfined compressive strengths were obtained using a strain rate of approximately 1 %/min for all specimens were obtained—according to ASTM D2166-06-. Corrections to the cross-sectional area were made prior to calculating the compressive stress on the specimen rendering to the standard. All tests were accomplished three times at least for each case. Curing time was a fundamental parameter for understanding the behavior of compacted disturbed cemented-soft clay; therefore, experimental schedule was arranged to perform the tests at different time periods (7, 28, 35, and 42 days) from mixing the clay with the cement.

Results and Discussion

Effect of Disturbance on the Stress Strain Behaviour

Figure 1 shows the difference in behaviour between disturbed and non-disturbed cemented clay for cement ratio, *aw* of 15 % tested after curing period, *t* of 28 days. For non-disturbed specimen, a clear brittle behaviour with peak strength and quite small residual strength can be also noticed with unconfined compressive strength, $q_{un\_Non\_28}$ of 270 kPa at axial strain at failure of 2 %, while the unconfined compressive strength for disturbed specimen, $q_{un\_D\_28}$ does not exceed 50 kPa regardless the compaction energy, and with failure stain of 6–7 % in a ductile behaviour with unclear peak strength.

The effect of compaction energy on the behaviour of disturbed cemented clay can be observed in Fig. 2 for the same conditions as in Fig. 1 (*aw* = 15 %, *t* = 28 days). The ductile behaviour for disturbed cemented clay changed to be more brittle with increasing the compaction energy. It can be noticed that the unconfined compressive strength increased with increasing the compaction energy, while the axial strain at failure decreased. For non-compacted specimen, the peak unconfined compressive strength, q_{un} was about 21 kPa at axial strain at failure of 12 %. However, the peak strength increased to 24 kPa with increasing the compaction energy to 460 kN m/m^3, where also the axial strain at failure reduced to 8 %, which reflects increasing the brittle behaviour with increasing the compaction

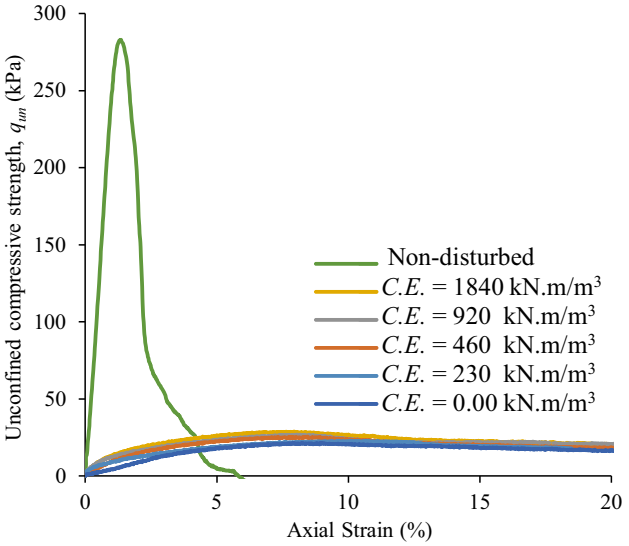

Fig. 1 Stress strain curve for disturbed and non-disturbed specimen (*aw* = 15 %, 28 curing days)

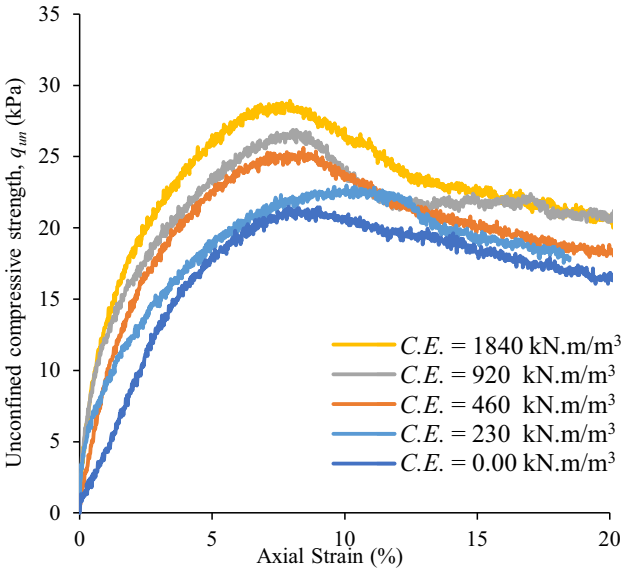

Fig. 2 Stress strain curve for disturbed specimen with different compaction energies (*aw* = 15 %, 28 curing days)

energy. The brittle behaviour became more clear for specimen compacted with higher dynamic energy, at compaction energy of 1840 kN m/m^3, the peak unconfined compressive strength reached 28 kPa with axial strain at failure of 6 %. Increasing the brittle behaviour can be explained due to understanding the effect of compaction energy on the soil unit weight as will be presented in Fig. 6, where increasing the soil unit weight will reflect as a reduction in the soil deformation and increasing in the brittle behaviour.

Effect of Curing Time on Both Unconfined Compressive and Modulus of Deformation

Figure 3 clarifies the variation of q_{un} under five different compaction energies with time for cement content of 15 %. Increasing the compaction energy reflected to a positive increasing in the unconfined compressive strength. At curing time of 28 days, q_{un} increased from 25 kPa at zero compaction energy to about 35 kPa at compaction energy of 1840 kN m/m^3 (i.e. the percentage of increasing is about 140 %). The same percentage of increasing can be also notice at curing time of 42 days, where q_{un} increased from 32 kPa to 46 kPa (increasing percentage of about 143 %) by increasing the compaction energy from zero to1840 kN m/m^3. It can be observed also that doubling the compaction energy from 920 to 1840 kN m/m^3 did not have the considerable effect on the compressive strength, where q_{un} at curing period of 28 days had increased from 33 to 35 kPa after increasing the compaction energy from 920 to 1840 kN m/m^3. The same trend can be noticed at curing time of 42 days, where increasing the compaction energy from 920 to 1840 kN m/m^3 effected on increasing the compressive strength from 43 to 46 kPa, i.e. increasing the compaction energy from 920 to 1840 kN m/m^3 caused an increasing in q_{un} with a percentage of 5–6 %. The unconfined compressive strength improved by percentages of 135, and 142 % by increasing the compaction energies from zero to 920 and from zero to 1840 kN m/m^3 respectively. This can be interpreted due to the high water content and the very low permeability of clay which affected the efficiency of compaction after certain compaction energy.

For more understanding to the effect of compaction energy and curing time on the disturbed cemented clay, Fig. 4 displays the effect of compaction energy on modulus of deformation, E_{50} for $aw = 15$ % with different curing periods, where E_{50} is the secant modulus of elasticity at 50 % of the unconfined compressive strength. It can be seen from the figure the increasing in modulus of deformation, E_{50} with increasing the compaction energy. At curing time of 28 days, E_{50} has increased from 1000 to 1250 kPa by increasing the compaction energy from zero to 920 kN m/m^3 and it has increased again to be 1500 kPa at compaction energy of 1840 kN m/m^3 with increasing percentage of 125 and 150 % for both compaction energies of 920 and 1840 kN m/m^3 respectively. The same trend still exists at curing period of 42 days, where E_{50} has augmented comparing the zero compaction case with increasing percentage of 123 and 142 % for both compaction energies of 920 and 1840 kN m/m^3 respectively.

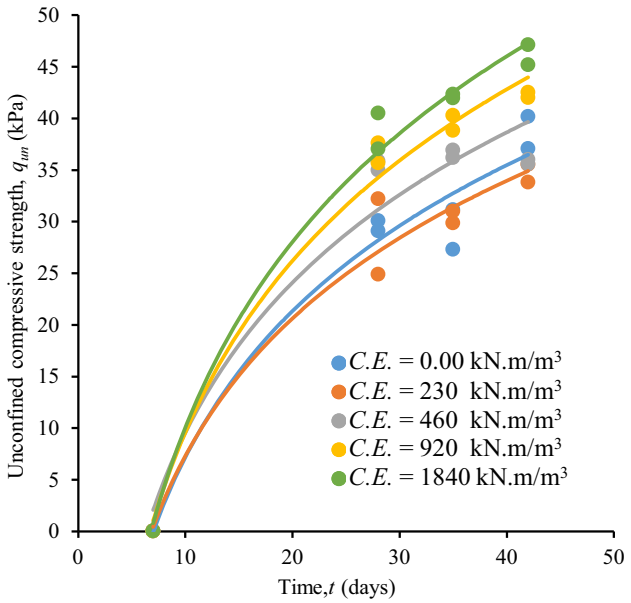

Fig. 3 Variation of unconfined compressive strength with time under different compaction energies ($aw = 15$ %)

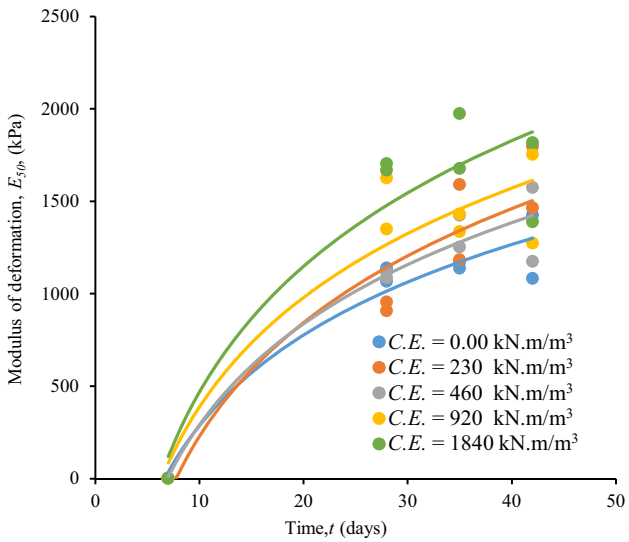

Fig. 4 Variation of modulus of deformation with time under different compaction energies ($aw = 15$ %)

Relationship Between Unconfined Compressive Strength and Modulus of Deformation for Both Disturbed and Non-Disturbed Specimens

According to previous studies [1, 22] for undisturbed cemented Japanese clays and Bangkok clay, it was found that E_{50} can be taken as approximate value of 50 to 300 × q_{un}. However, in this study the correlation value of E_{50} can be considered as 160 q_{un} ($R^2 = 0.89$) as it can be seen in Fig. 5a. This difference between the current study and the previous studies can be explained due to the difference in used clay and water content, however both values can be acceptable to estimate E_{50} from the corresponding q_{un}.

Figure 5b shows the relation between E_{50} and the corresponding q_{un} for disturbed compacted cemented clay with different cement ratios and different compaction energies. As mentioned before in Fig. 1, that the disturbance process reduced the unconfined compressive strength of the cemented clay and transferred the behaviour to be ductile, this behaviour can be seen clearly form the approximate function between E_{50} and the corresponding q_{un}. The multiplier factor to estimate E_{50} has considerably reduced from ($E_{50} = 160\ q_{un}$) for non-disturbance cemented clay to ($E_{50\_D} = 25 - 50\ q_{un\_D}$) for disturbance cemented clay.

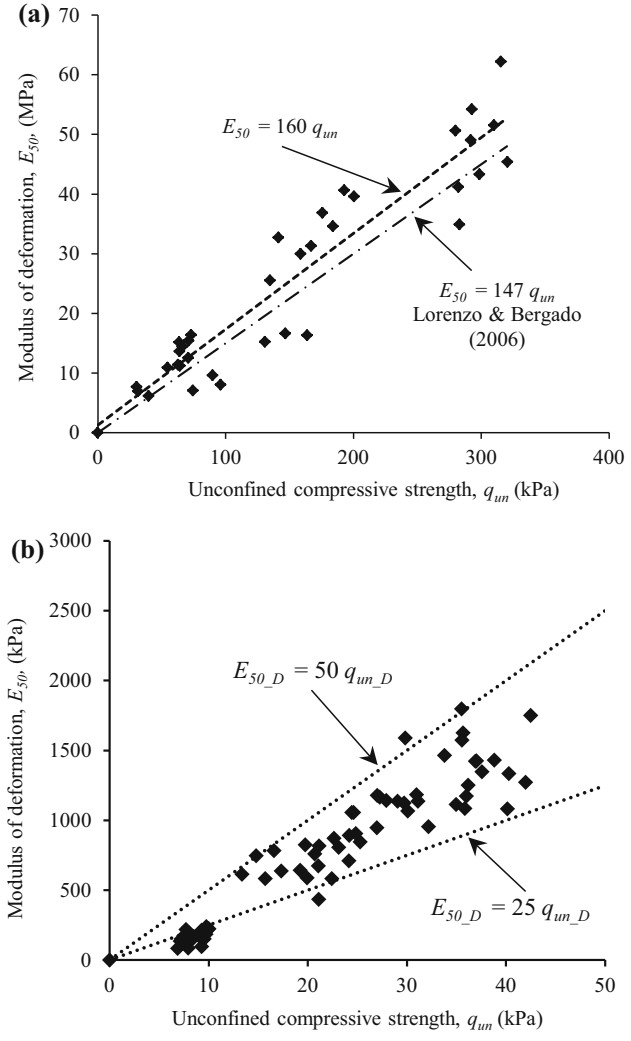

Fig. 5 Modulus of deformation versus unconfined compressive strength of: **a** non-disturbed cemented clay; **b** disturbed cemented clay

Effect of Compaction Energy on Dry Unit Weight

The plot of dry unit weight against compaction energy for various cement ratios is shown in Fig. 6, where increasing the soil unit weight is the key target for compaction process. Increasing the soil unit weight will lead to reduction in the ground settlement, increasing in shear strength, and increasing in the bearing capacity. From Fig. 6, increasing the compaction energy affected positively on dry unit weight, where the average dry unit weight—at $aw = 10$ %—has increased from 7.0 to 7.3 kN/m^3 by increasing the compaction energy from zero to 460 kN m/m^3, and has reached 7.5 kN/m^3 at compaction energy level of 920 kN m/m^3. Increasing dry unit weight with increasing the compaction energy was expected due to the effect of compaction on reducing void space between particles, which leaded to increasing in the unit weight and increasing in the brittle behaviour of the soil as shown in Fig. 2. However, the compaction efficiency can affect by some factors such as soil permeability and water content, where it can be noticed at low level of compaction energy. Increasing the compaction energy from zero to 230 kN m/m^3 did not have the noticeable effect on increasing the dry unit weight, while this effect started to be obvious at starting from compaction energy of 460 kN m/m^3. This can be explained from the interaction between clay-cement

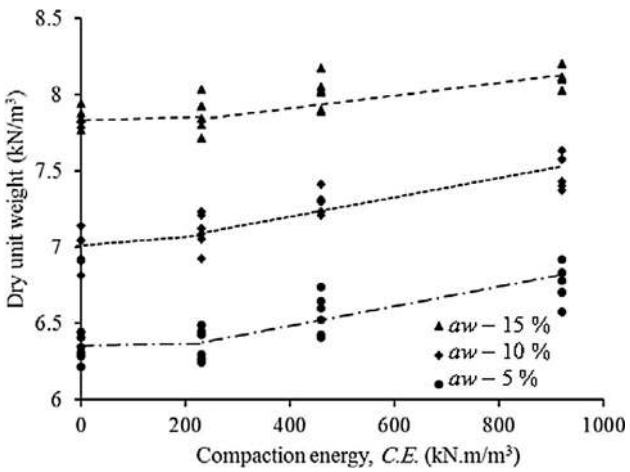

Fig. 6 Effect of compaction energy on dry unit weight

clusters and water inside the soil gaps. When cement mixed with soft clay, cement and clay particles group together to form a large clay-cement clusters, reducing the soil permeability [23]. Where low compaction energies (less than 230 kN m/m^3) are not enough to push the water trapped inside the soil matrixes to get outside, which will reduce the pore holes' size and increase the unit weight. While for high compaction energies (more than 230 kN m/m^3), increasing the compaction energy will increase the amount of water expels from inside the soil pore holes, which will increase the soil unit weight as well. Cement content affected the dry unit weight, where increasing the cement content was followed by raising in the dry unit weight. Dry unit weight increased from 6.7 to 7.5 kN/m^3 by increasing *aw* from 5 to 10 %, and to 8.1 kN/m^3 at *aw* of 15 %. This can be explained due to increasing the cemented pozzolanic formations inside the soil gaps, which increased by increasing the cement ratio.

Relationship Between Unconfined Compressive Strength and Both Dry Unit Weight and Voids Ratio

Figure 7 displays the relationship between dry unit weight and disturbed unconfined compressive strength for different cement ratios. This relationship was effected by changing the cement content, and this can be noticed clearly from the slope of the three trend lines (A, B and C). The slope of trend line A with the horizontal projection is almost neglectable, which means that changing the dry unit weight does not have considerable effect on q_{un} for $aw = 5$ %, where the dry unit weight changed from 6.3 to 6.9 kN/m^3 with average change in q_{un} was from 6.5 to 8.5 kPa. The slope of trend line B is more apparent than the trend line A, which clarifies the relationship between dry unit weight and q_{un_D} for $aw = 10$ %, where the average dry unit weight has changed from 6.9 to 7.7 kN/m^3 accompanied by changing in q_{un_D} from 15 to 27 kPa. That relationship reached the utmost clarity in case of trend line C ($aw = 15$ %), where the changing in dry unit weight—just from 7.8 to 8.2 kN/m^3—was followed by high changing in q_{un_D}—from 26 to more than 40 kPa.

The final void ratio, *e* corresponding to each dry unit weight—which takes into consideration the effect of water content, and compaction energy—can be calculated as follows:

$$e = \frac{(1 + wc) \times G_s \times \gamma_w}{\gamma_t} - 1 \quad (1)$$

where γ_t = the total unit weight after curing, wc = the water content corresponding to γ_t, γ_w = water unit weight, and G_s = the mixture specific gravity.

The formation of *e*/*aw* has already collected the effect of several variables such as water content, cement ratio, and compaction energy. The reason behind the division of *e* by *aw* that some specimens can have different cement ratios and compaction energies, however it may chance to have the same void ratio, and for sure not the same value of q_{un_D}. The following empirical relationship has been delivered to estimate the value of q_{un_D} as clear in Fig. 8:

$$q_{un\_D} = 700 \times {}^{e}/_{aw} \quad (2)$$

Estimating the Value of the Increasing Factor *i*

It is important to find a strategy to estimate both unconfined compressive strength and modulus of deformation for disturbed cemented clay under different compaction

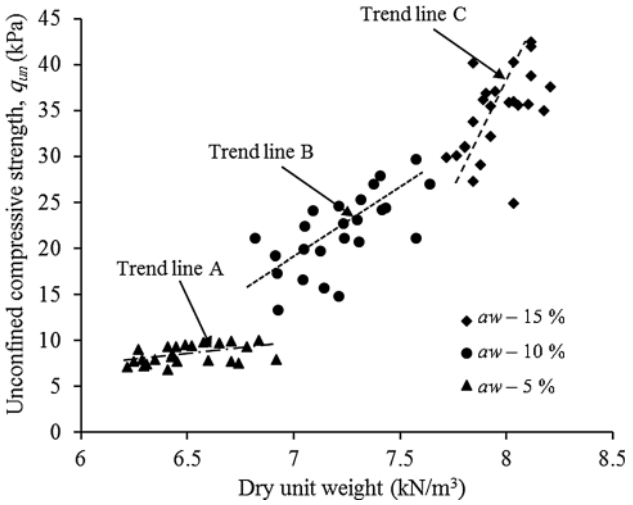

Fig. 7 Relationship between dry unit weight and disturbed unconfined compressive strength

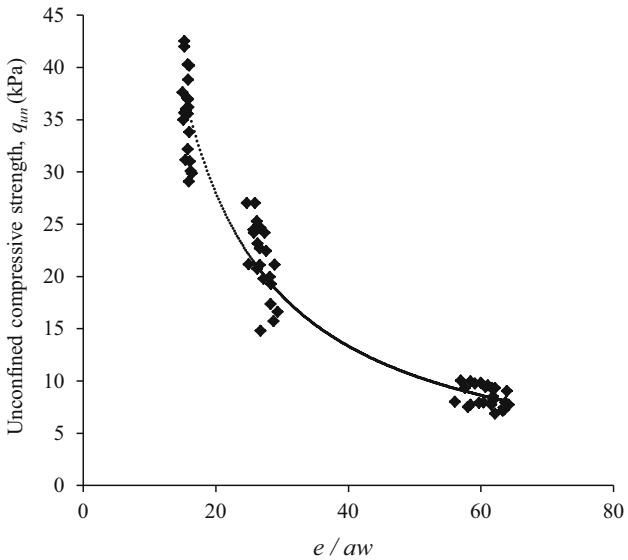

Fig. 8 Unconfined compressive strength versus *e*/*aw*

energies for various curing periods. A clear relationship between unconfined compressive strength for non-disturbed specimens at curing time t, $q_{un\_Non\_t}$ and unconfined compressive strength for disturbed non compacted specimens at the same curing time t, $q_{un\_D\_T\_t}$ can be figured out from Fig. 9, where it can be written as following:

$$q_{un\_D\_T\_t} = 0.1 \times q_{un\_Non\_t} \quad (3)$$

where both $q_{un\_Non\_t}$ and $q_{un\_D\_T\_t}$ have the same cement ratio, water content and curing time.

For disturbed cemented clay, the unconfined compressive strength will increase than q_{un_D} with increasing the compaction energy as mentioned before in Fig. 2. This increasing can be represented by the factor i, as following:

$$q_{un\_D\_comp\_i} = i \times q_{un\_D\_28} \quad (4)$$

where $q_{un\_D\_comp\_t}$ is the unconfined compressive strength for disturbed cemented clay under compaction energy, after curing period of t, $q_{un\_D\_T\_28}$ is the unconfined compressive strength for disturbed cemented non compacted clay after 28 days curing period for the same cement ratio and i is the increasing factor as percentage.

It was not possible to figure out a formula to estimate i statistically, thus using neural network tool will be essential to estimate the value of i as a function of both curing time and compaction energy.

Artificial Neural Network

Artificial Neural Network, *ANN* is a mathematical tool which represents the neurological function of the brain. *ANN* can simulate the brain learning method by creating a mesh interconnection between cells mathematically. It is a great tool to model such problems where the constraints which rule the outcomes are complicated. It is also capable of defining the collaborative effects for different variables in a complex process. *ANN* can model the complicated relations among inputs and outputs without needing for a detailed mechanical explanation of the phenomena that control the process. *ANN* has a lot of applications in geotechnical engineering such as deep foundation behaviour [24–27], mechanical behaviour of soils [28–32], tunneling and underground structures [33], site investigation, settlement [34, 35] and soil liquefaction [36, 37].

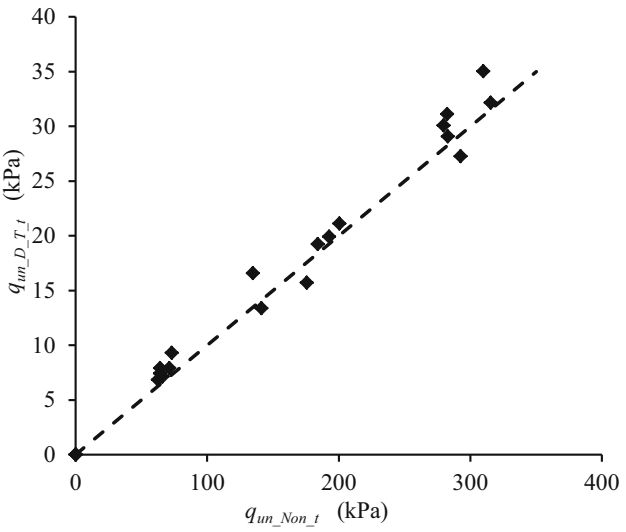

Fig. 9 Unconfined compressive strength for non-disturbed specimens versus unconfined compressive strength for disturbed non compacted specimens

A neural network consists of input layers, hidden layers, and an output layer. In hidden layers, neurons are using weights to connect to other neurons in both input and output. These neurons enable the network to perform complicated relations among inputs and output variables. The model training is determining the weights and this stage is similar to identify the polynomial coefficients in regression analysis. At the first the weights are chosen at random, and then an iterative algorithm is used to discover the needed weights to reduce the variances between -calculated and actual outputs [38].

To predict value of i, a feed forward *ANN* was considered and the selected input parameters were curing time in days, and compaction energy in kN m/m^3. The input layer consisted of two neurons (curing time, and compaction energy), while the ratio of increasing the stress i was the only neuron in the output layer. Eighty data points for three cement ratios, three curing times and five compaction energies values were used for the neural network model. The data was then used to train the ANN by randomly utilizing 70, 15, and 15 % of the data for training, validation, and testing, respectively. As the number of parameters is much smaller than the total number of training points, then there is little or no chance of overfitting. At the first various numbers of neurons were tested for a single hidden layer model but it was not accurate enough as it showed low correlation. Thus, a hidden double layer model was chosen. Different trials were considered to decide the suitable neurons number in both hidden layers. Figure 10 displays the values of coefficient of determination, R^2 between both experimental and predicted output for several neurons numbers in both hidden layers where, the highest coefficient of determination which is the result of using 8 neurons in both first and second hidden layers. From the literature, if the neurons number in both hidden layers is greater than the optimal, the model will be complicated and the training time will be longer [38].

Neurons in both hidden layers were non-linear with a sigmoid transfer function. Figure 11 demonstrations *ANN* configuration and the used transfer functions among the network layers. *ANN* was trained using *Matlab platform*

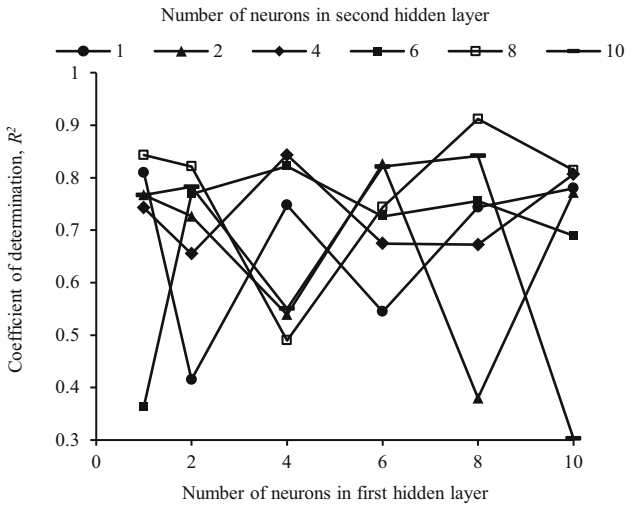

Fig. 10 Coefficient of determination for various numbers of neurons for both hidden layers

R2009. The used algorithm in this model was a feed forward algorithm. Feed forward algorithm adjusted the weights to decrease the error and this process was repeated until the error between both experimental and predicted output satisfied certain error criterion.

The weight and bias matrices found after training the *ANN* model are:

W_1 =		B_1 =
3.52	2.32	−3.62
−3.05	2.74	2.67
3.78	1.25	−1.68
−3.31	−2.22	0.59
−2.40	−3.11	−0.50

W_1 =			B_1 =
−3.61		−1.57	−1.83
1.06		3.87	2.79
3.42		−2.05	3.93

W_2 =								B_2 =
−0.01	0.27	−0.77	−0.27	−0.96	0.25	−1.31	0.30	−1.69
−0.59	0.41	−0.30	−0.87	0.63	0.56	0.67	−0.69	1.41
−0.51	0.61	1.29	0.37	−0.56	0.10	−0.21	−0.39	1.10
−0.39	−0.68	−0.48	−0.17	0.86	−0.97	−0.02	−0.60	0.03
−0.58	−1.16	−0.71	−0.38	0.50	0.12	0.86	0.31	−0.05
0.95	−0.71	−0.07	−1.21	−0.55	0.68	0.54	0.26	0.50
0.75	−0.58	−0.25	0.56	0.91	0.51	−1.09	−0.78	1.11
0.96	−0.89	0.64	−0.16	0.10	0.32	0.70	0.82	1.73

W_3 =								B_3 =
−0.38	−0.73	−0.04	−0.47	0.21	−0.31	−0.41	0.22	−0.264

where W_1 is a matrix which represents the connection weights between neurons in input layer and first hidden layer, W_2 is a matrix which represents the connection weights between neurons in first and second hidden layer neurons, W_3 which represents the connection weights between neurons in second and output layer neurons, B_1 and B_2 are the bias matrixes for the hidden layers 1 and 2 respectively, and B_3 is the bias matrix for the output layer neurons. The normalized Y_n for i can be calculated as in following equations:

$$Y_n = W_3 \times (\log\mathrm{sig}(W_2 \times (\log\mathrm{sig}(W_1 \times X_n + B_1)) + B_2)) + B_3 \quad (5)$$

$$\log\mathrm{sig}(X) = 1/(1 + \exp(-X)) \quad (6)$$

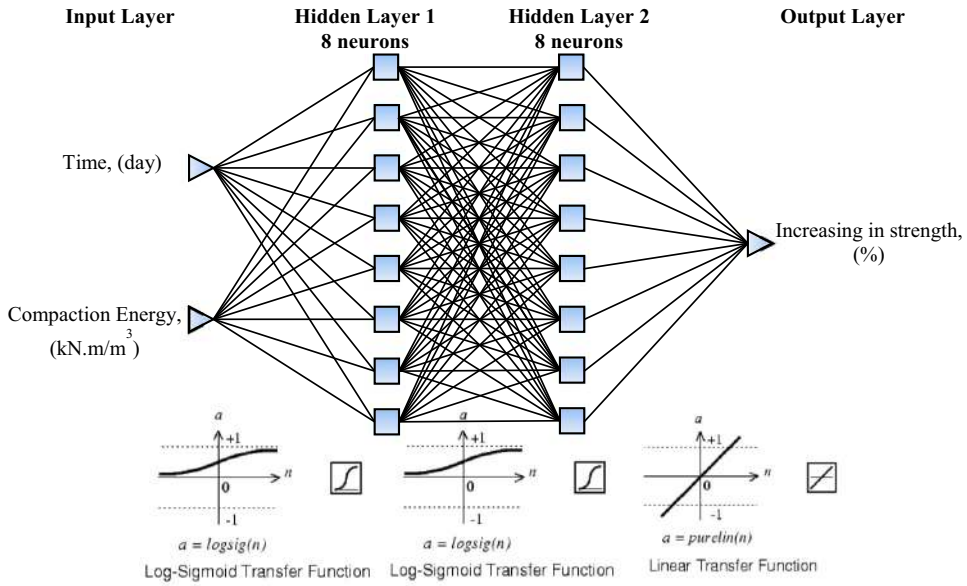

Fig. 11 Artificial Neural Network (*ANN*) configurations

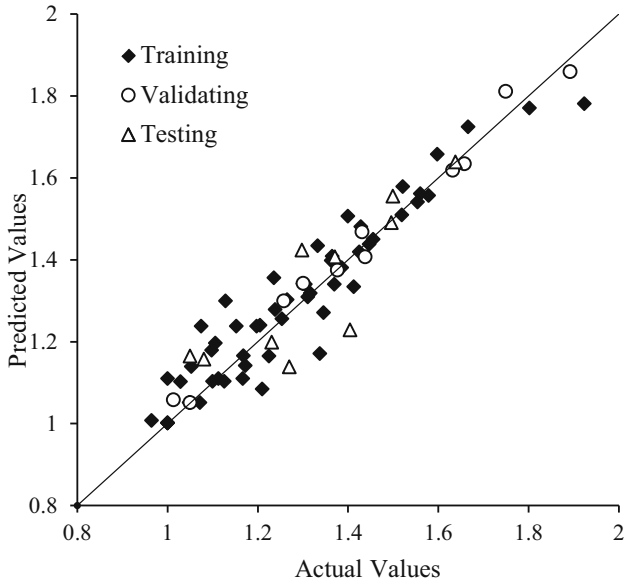

Fig. 12 Correlation between experimental and *ANN*-predicted for increasing percentage, *i*

Figure 12 presents the correlation between both experimental and predicted for *i* from *ANN* model for data points used for training, validating, and testing the model.

Conclusions

This study focuses on investigating the behavior compacted disturbed cemented soft clay under different compaction energies and curing periods. Three different cement contents are used in this study with water content of about 120 %. Within the experimental range of this investigation, the following conclusions can be drawn:

- Disturbing the soil has a serious effect on the stress strain behaviour, where the behaviour changes from being brittle with peak to more ductile, with a huge reduction in the compressive strength and modulus of deformation.
- The stress strain behavior has changed slightly due to the compaction, where increasing the compaction energy changed the behaviour to be more brittle with increasing both unconfined compressive strength, q_{un} and modulus of deformation, E_{50}. The relationship between q_{un} and E_{50} for undisturbed cemented clay has an acceptable matching with the previous test results.
- Increasing the compaction energy reflects to increase the soil dry unit weight, however the compaction mechanism can affect by some factors such as high water content and soil particles size especially at low levels of compaction energy.
- The relationship between unconfined compressive strength, q_{un} and both dry unit weight and voids ratio affects by many factors such as the cement ratio, water content, and the compaction energy, therefore using the term *e*/*aw* can be more reliable to relate q_{un} with the soil void ratio *e*.
- Obtaining a formula for the increasing factor *i* shall be helpful to estimate the value of unconfined compressive strength for disturbed cement clay for different cement ratio, compaction energy, and curing time.
- *ANN* is excellent tool for modeling the increasing factor *i* including different variables (compaction energy and curing period) with high correlation between experimental and predicted data
- R^2 of 0.924, 0.908, and 0.889 were achieved for training, validating, and testing data points, respectively, with average R^2 of 0.916.

Acknowledgments The first author wishes to express his gratitude to Tokyo Institute of Technology for providing the needed materials and apparatuses where this work would not have been possible without that valuable support.

References

1. Ministry of Transport, The Fifth District Port Construction Bureaus, "Pneumatic flow mixing method", Yasuki Publishers, 157 pp (in Japanese)
2. Kitazume M, Hayano K (2007) Strength properties and variance of cement-treated ground using the pneumatic flow mixing method. Proc Inst Civ Eng—Gr Improv 11(1):21–26
3. Kitazume M, Satoh T (2003) Development of a pneumatic flow mixing method and its application to Central Japan International Airport construction. Proc Inst Civ Eng—Gr Improv 7(3):139–148
4. Kitazume M, Satoh T (2005) Quality control in Central Japan International Airport construction. Proc Inst Civ Eng—Gr Improv 9(2):59–66
5. Yamauchi H, Ishiyama Y, Oonishi F (2011) Study for beneficial use of soft dredged soil—case history of back fill behind the breakwater at Kushiro Port. In: Proc. Annu. Tech. Meet. Civ. Eng. Res. Inst. Cold Reg. (in Japanese)
6. Horpibulsuk S, Miura N, Nagaraj T (2003) Assessment of strength development in cement-admixed high water content clays with Abrams' law as a basis. Geotechnique 53(4):439–444
7. Horpibulsuk S, Miura N, Bergado DT (2004) Undrained shear behavior of cement admixed clay at high water content. J Geotech Geoenviron Eng 130(10):1096–1105
8. Horpibulsuk S, Liu MD, Liyanapathirana DS, Suebsuk J (2010) Behaviour of cemented clay simulated via the theoretical framework of the structured cam clay model. Comput Geotech 37(1–2):1–9
9. Horpibulsuk S, Rachan R, Suddeepong A, Liu MD, Jun Y (2013) Compressibility of lightweight cemented clays. Eng Geol 159:59–66
10. Horpibulsuk S, Wijitchot A, Nerimitknornburee A, Shen SL, Suksiripattanapong C, Al SHET (2014) Factors influencing density and strength of lightweight cemented clay. Q J Eng Geol Hydrogeol 47:101–109

11. Horpibulsuk S, Liu MD, Liyanapat hirana J, Suebsuk DS (2010) Behavior of cemented clay simulated via the theoretical framework of the structured cam clay model. Comput Geotech 37:1–9
12. Horpibulsuk S, Rachan R, Suddeepong A, Chinkulkijniwat A (2011) Strength development in cement admixed Bangkok clay: laboratory and field investigations. Soils Found 51:239–251
13. Horpibulsuk S, Suddeepong A, Chinkulkijniwat A, Liu MD (2012) Strength and compressibility of lightweight cemented clays. J Appl Clay Sci 69:11–21
14. Horpibulsuk S, Chinkulkijniwat A, Cholphatsorn A, Suebsuk J, Liu MD (2012) Consolidation behavior of soil cement column improved ground. Comput Geotech 43:37–50
15. Askarani KK, Pakbaz MS (2016) Drained shear strength of over-consolidated compacted soil-cement. J Mater Civ Eng 28(5)
16. Pakbaz R, Alipour MS (2012) Influence of cement addition on the geotechnical propertis of an Iranian clay. J Appl Clay Sci 67:1–4
17. Pakbaz MS, Farzi M (2015) Comparison of the effect of mixing methods (dry versus wet) on mechanical and hydraulic properties of treated soil with cement lime. J Appl Clay Sci 105:156–169
18. Boroumandzadeh B, Pakbaz MS (2012) Evaluation of effect of cementation on drained shear strength of over consolidated clay soils. World Appl Sci J 16(10):1375–1379
19. Neville AM (1997) Properties of concrete: fourth and final edition. Wiley
20. ECP 203 (2009) Egyptian code for designing and executing the building works, 2nd edn. HBRC, Egypt
21. J. G. Society (2009) Practice for making and curing stabilized soil specimens without compaction. JGS 0821-2009 Jpn Geotech Soc 1:426–434 **(in Japanese)**
22. Lorenzo GA, Bergado DT (2006) Fundamental characteristics of cement-admixed clay in deep mixing. J Mater Civ Eng 18(2):161–174
23. Horpibulsuk S, Rachan R, Raksachon Y (2009) Role of fly ash on strength and microstructure devlopment in blended cement stabilized silty clay. Soils Found 49(1):85–98
24. Abu-Kiefa MA (1998) General regression neural networks for driven piles in cohesionless soils. J Geotech Geoenviron Eng 124(12):1177–1185
25. Lee I-M, Lee J-H (1996) Prediction of pile bearing capacity using artificial neural networks. Comput Geotech 18(3):189–200
26. Teh CI, Wong KS, Goh ATC, Jaritngam S (1997) Prediction of pile capacity using neural networks. J Comput Civ Eng 11(2):129–138
27. Das SK, Basudhar PK (2006) Undrained lateral load capacity of piles in clay using artificial neural network. Comput Geotech 33(8):454–459
28. Penumadu D, Zhao R (1999) Triaxial compression behavior of sand and gravel using artificial neural networks (ANN). Comput Geotech 24(3):207–230
29. Ellis GW, Yao C, Zhao R, Penumadu D (1995) Stress–strain modeling of sands using artificial neural networks. J Geotech Eng 121(5):429–435
30. Chittoori B, Puppala AJ (2011) Quantitative estimation of clay mineralogy in fine-grained soils. J Geotech Geoenviron Eng 137(11):997–1008
31. Das SK, Basudhar PK (2008) Prediction of residual friction angle of clays using artifical neural network. Eng Geol 100(3–4):142–145
32. Das SK (2012) Artificial neural networks in geotechnical engineering: modeling and application issues, Chapter 10. Metaheuristics Water, Geotech. Transp. Eng., pp 231–270
33. Benardos AG, Kaliampakos DC (2004) Modelling TBM performance with artificial neural networks. Tunn Undergr Sp Technol 19:597–605
34. Shahin MA, Jaksa MB, Maier HR (2001) Artificial neural network applications in geotechnical engineering. Aust Geomech 36(1):49–62
35. Sivakugan N, Eckersley JD, Li (1998) Settlement predictions using neural networks. Aust Civ Eng Trans CE40:49–52
36. Goh ATC (1994) Seismic liquefaction potential assessed by neural network. J Geotech Geoenviron Eng 120(9):1467–1480
37. Goh ATC (1996) Neural-network modeling of CPT seismic liquefaction data. J Geotech Eng 122(1):70–73
38. Nasr N, Hafez H, El Naggar MH, Nakhla G (2013) Application of artificial neural networks for modeling of biohydrogen production. Int J Hydrogen Energy 38(8):3189–3195